Highly Efficient Red Phosphorescent OLEDs Employing a Multifunctional Oligofluorene Host

Ming-Han Tsai[1], Hai-Ching Su[1], Chung-Chih Wu[1], Ken-Tsung Wong[2], Wen-Ren Li[3]*

[1]Department of Electrical Engineering and Graduate Institute of Electro-optical Engineering, National Taiwan University, Taipei, Taiwan
*TEL:+886-2-23635251 ext 346, e-mail: chungwu@cc.ee.ntu.edu.tw
[2]Department of Chemistry, National Taiwan University, Taipei, Taiwan
[3]Department of Chemistry, National Central University, Chung-Li, Taiwan

Keywords: high efficiency, phosphorescence, red, OLED.

Abstract

High-efficiency red phosphorescent OLEDs employing a novel red emitter and a multifunctional oligofluorene host are reported. With qazIr(acac) as the red phosphorescent dopant, a maximum external quantum efficiency of 19% and maximum power efficiency of 11 lm/W are achieved. In addition, single layer devices using such host and dopant materials have efficiencies up to 13%.

1. Introduction

The efficiencies of organic light-emitting devices (OLEDs) have advanced rapidly in recent years due to development of efficient phosphorescent dopant molecules containing transition metals that can harvest both electro-generated singlet and triplet excitons for emission. In the research of red phosphorescent OLEDs, various phosphorescent dopants and device structures have been developed. Several commonly known examples of red phosphorescent dopants include PtOEP, btpIr(acac), Irpiq, along with their analogues. As for device structures, the usage of CBP as host and BCP as hole-blocking/exciton-blocking layer is most general. However, unlike green phosphorescent OLEDs which are already known to achieve nearly 100% internal quantum efficiency, effort is still need to be paid to improve the performances of red phosphorescent OLEDs. To fabricate highly efficient red phosphorescent OLEDs, it is necessary to search for red-emissive metal complexes with large luminescence quantum yields. In this study, a novel red phosphorescent dopant qazIr(acac) is adopted, with qaz and acac representing 4-((2R,6S)-2,6-dimethylpiperidin-1-yl)-2-(thiophen-2-yl)quinazoline

and acetylacetonate ligands, respectively. Devices using such a dopant achieve a high external quantum efficiency of nearly 20%.

To achieve a phosphorescent device with good performance, in addition to efficient emitting dopants, there are several requirements for the host material as well, such as a sufficiently large triplet energy, appropriate carrier mobility and morphological stability. The triplet energy of the host has to be larger than that of the dopant to prohibit reverse energy
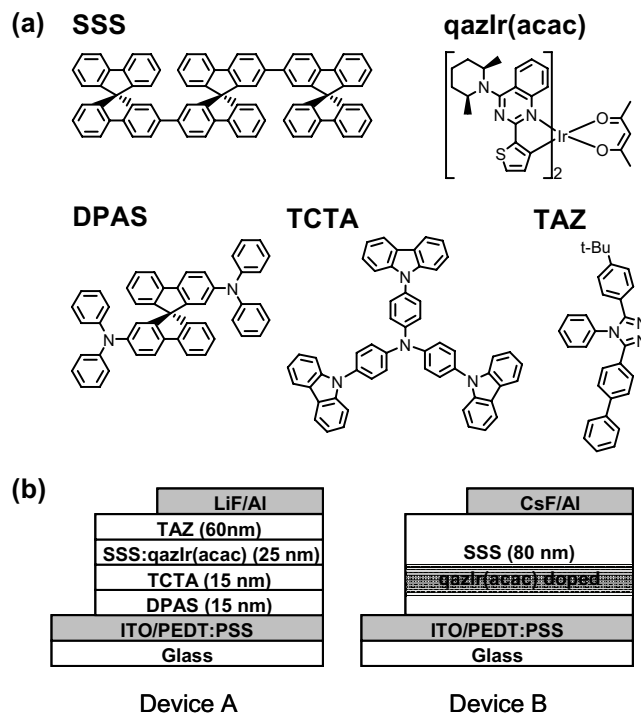

Figure 1. (a) Chemical structures of the materials used in this study. (b) Designed multilayer and single layer device structures.

transfer from the dopant back to the host and effectively confine the triplet excitons on the dopants. Carrier-transport characteristics influence the position of the exciton formation zone and the recombination processes. High glass transition temperature and thus a stable morphology are required to achieve a long operational lifetime of devices. In this work, an improved red phosphorescent device employing a novel oligofluorene host SSS is reported. In addition to merely acting as a host material in a multilayer device, SSS is also capable of functioning as the hole transporting layer and electron transporting layer by itself, due to the ambipolar carrier transporting properties of oligofluorenes. In other words, SSS makes possible the fabrication of an efficient single layer device.

Single layer devices strongly benefit the simplification of the fabrication processes, and also reduces device aging and the excess voltage drops across material interfaces. Several attempts have been made to realize single layer small-molecule OLEDs, however the results were not entirely superb. In this paper, a highly efficient single layer small-molecule OLED with impressive performances is demonstrated. Such an achievement is made by the usage of an intrinsically ambipolar host material and a novel efficient phosphorescent dopant, and also the judicious selection of carrier injection interfaces.

2. Results and discussion

Figure 1(a) shows the chemical structures of qazIr(acac) and SSS. The room-temperature (RT) UV-Vis absorption spectrum and photoluminescent (PL) spectra of qazIr(acac) in toluene solution at RT and 77 K are shown in Figure 2(a). The strong absorption in the UV region with the molar absorption coefficient ε >20000 $M^{-1}cm^{-1}$ is assigned to the spin-allowed $^1\pi$-π^* transition of the ligands. Broad and weaker absorption bands of qazIr(acac) are in the wavelength region longer than 400 nm. Broad absorption shoulders appear at ~430 nm and ~550 nm, with ε ~10000 $M^{-1}cm^{-1}$ and ~1000 $M^{-1}cm^{-1}$, respectively. These are likely to be ascribed to the singlet metal-to-ligand charge-transfer (^{1}MLCT) and triplet metal-to-ligand charge-transfer (^{3}MLCT) transitions, respectively. The Stokes shift between the ^{3}MLCT and emission bands observed here is rather small, which is the case when the emission is from a predominantly ^{3}MLCT state. The measured lifetime at room temperature is 0.22 µs, also indicating a strong spin-orbital coupling. From Figure 2(a) it can be observed that the PL spectrum
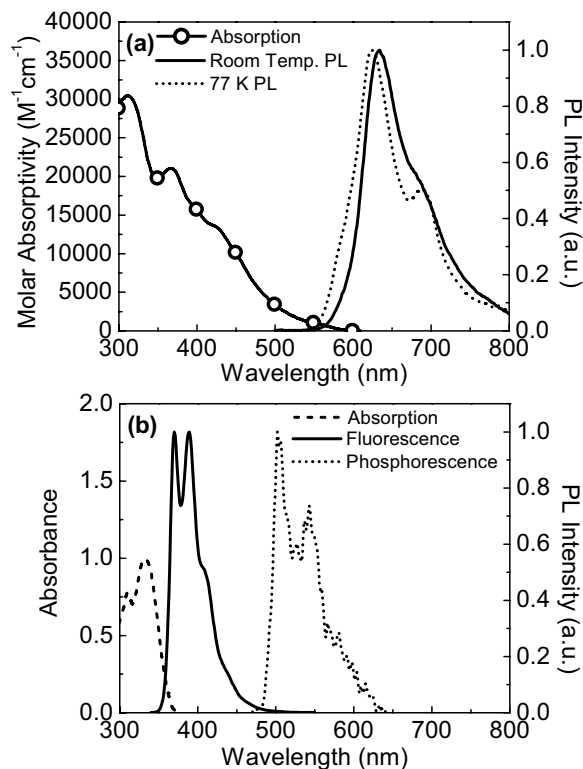

Figure 2. (a) The room-temperature (RT) absorption spectrum and PL spectra of qazIr(acac) in toluene solution at RT and 77 K. (b) RT absorption, fluorescence and 77 K phosphorescence spectra of SSS in toluene.

measured at RT is broad and that measured at 77 K lacks fine vibronic progressions, which again suggests that lowest excited triplet state of qazIr(acac) gains dominant contributions from the ^{3}MLCT state.

Linking two bifluorene moieties through spiro-configuration is significantly beneficial to the thermal stability and morphological stability. Thermogravimetric analysis (TGA) indicates that spiro-bridged bifluorenes SSS exhibits a decomposition temperature (T_d, corresponding to 10% weight loss) as high as 464 °C. In differential scanning calorimetry (DSC), SSS exhibits an extinct glass transition temperature (T_g) up to 228 °C. With a high T_g and thus resistance against crystallization, SSS is able to form homogeneous and stable amorphous films by thermal evaporation. Figure 2(b) shows the RT absorption, fluorescence and 77 K phosphorescence spectra of SSS in dilute toluene solution. By taking the highest-energy peak of phosphorescence as the transition energy of $T_1 \rightarrow S_0$, the triplet energy of SSS is estimated to be about 2.5 eV. This indicates that it may be used as an efficient host for yellow to red phosphorescent emitters. In addition, to achieve efficient energy transfer between

Table 1. The HOMO and LUMO energy levels based on the cyclic voltammetry for qazIr(acac) and SSS.

Compound	HOMO energy level (eV)	LUMO energy level (eV)
qazIr(acac)	4.98	2.42
SSS	5.76	1.98

the host and the phosphorescent dopant, spectral overlap between the emission spectrum of the host and the absorption spectrum of the dopant is required. As shown in Figure 2, there is sufficient overlapping between the absorption spectrum of qazIr(acac) and the fluorescence and phosphorescence spectra of SSS, satisfying the iso-energy requirement for efficient energy transfer.

As mentioned in above, the electro-generated excitons should eventually all recombine on the phosphorescent dopant sites in order to obtain efficient phosphorescent devices. There are generally two pathways regarding this process. One is that the holes and electrons form excitons on host molecules and subsequently be energy-transferred to dopant sites. The other pathway is that the excitons directly form on dopants. For the first situation, sufficient spectral overlapping is required, as discussed in above. As for the second situation, the energy levels of the highest occupied molecular orbital (HOMO) and the lowest unoccupied molecular orbital (LUMO) of the host and dopant needs particular attention in order to ensure that the dopant effectively traps both carriers for the formation of excitons. Therefore cyclic voltammetry (CV) measurements were carried out to study the relative energy level positions of SSS and qazIr(acac). Both compounds were found to undergo both reversible anodic oxidation and cathodic reduction to form stable cation and anion radicals, respectively. It is expected that SSS and qazIr(acac) will be stable when accepting holes and electrons in OLEDs. Table 1 summarizes the oxidation and reduction potentials, HOMO and LUMO energy levels for SSS and qazIr(acac), based on the cyclic voltammetry. The energy level difference between the HOMOs of SSS (5.76 eV) and qazIr(acac) (4.98 eV) is ~0.8 eV, while the difference between the LUMOs of SSS (1.98eV) and qazIr(acac) (2.42 eV) is ~0.4 eV. It can be seen that both energy differences are considerably large. Therefore qazIr(acac) is expected to be capable of effectively trapping both holes and electrons in SSS to directly form excitons, if this pathway is to contribute to the exciton formation process.

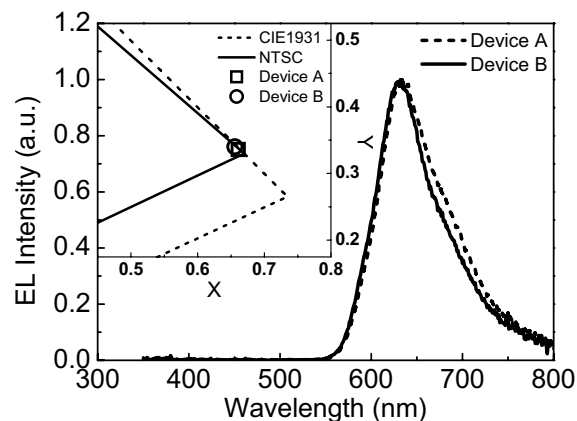Therefore SSS and qazIr(acac) are considered to be

Figure 3. The EL spectra of Device A and Device B. The inset shows the CIE1931 chromaticity coordinates of the two devices.

promising host and dopant materials for red electrophosphorescence. The devices were fabricated on glass substrates with the typical structure of multiple organic layers sandwiched between the bottom indium tin oxide (ITO) anode and the top metal cathode (Al). The fabricated Device A uses a structure of ITO/PEDT:PSS (~30 nm)/DPAS (15 nm)/TCTA (15 nm)/SSS doped with 8 wt.% qazIr(acac) (25 nm)/TAZ (60 nm)/LiF (0.5 nm)/Al, where the conducting polymer polyethylene dioxythiophene/polystyrene sulphonate (PEDT:PSS) was used as the hole-injection layer, 2,2'-bis(N,N-diphenylamine)-9,9'-spirobifluorene (DPAS) and 4,4',4''-tri(*N*-carbazolyl)triphenylamine (TCTA) as the hole-transport layers, SSS doped with qazIr(acac) as the emitting layer, 3-(4-biphenylyl)-4-phenyl-5-(4-*tert*-butylphenyl)-1,2,4-triazole (TAZ) as the electron-transport layer, and LiF as the electron-injection layer. Chemical structures of related compounds are shown in Figure 1(a) and the device structure in Figure 1(b).

As shown in Figure 3, electroluminescence (EL) of Device A only shows emission from qazIr(acac), indicating the effective confinement of triplet excitons on the phosphorescent dopants and the effective injection of both holes and electrons into the emitting layer. The CIE1931 coordinates of the red device is (0.661, 0.336). I-V-L characteristics and external EL quantum efficiency of the device are shown in Figure 4(a) and Figure 4(b). A luminance of 17 cd/m^2 was obtained at J = 0.1 mA/cm^2 and the maximum luminance was 32000 cd/m^2 obtained at 18.5 V. A high external EL quantum efficiency of 18.8% photon/electron (15.2 cd/A, maximum) and a maximum power efficiency of 10.5 lm/W were observed. Assuming an outcoupling efficiency of ~20%, the internal quantum efficiency is nearly 100%.
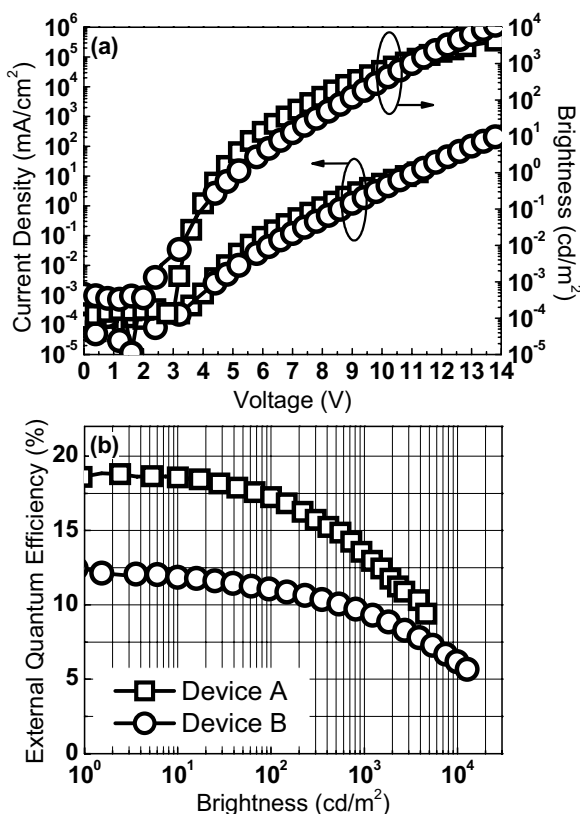
Figure 4. (a) I-V-L characteristics, and (b) external EL quantum efficiency vs. brightness of Device A and B.

Efficiency roll-off at higher currents, typical in phosphorescent OLEDs and associated with triplet-triplet annihilation, is also observed here, yet at the practical brightness of 100 cd/m^2, the efficiencies remain above 17.2%, 14.0 cd/A and 5.6 lm/W.

The ambipolar carrier transporting properties typical in oligofluorenes is attractive considering the application in single layer devices. Therefore Device B with a single layer structure was fabricated: ITO/PEDT:PSS/SSS partially doped with 8 wt.% qazIr(acac) (80 nm)/CsF (1 nm)/Al, where the emitting region is 20 nm of SSS doped with 8 wt.% qazIr(acac) located 40 nm from the cathode, and SSS functions as the hole-transport and electron-transport layers itself. CsF is used as the electron-injection layer. The host SSS is not entirely doped in order to prevent the excitons from diffusing to the electrodes, which might act as quenching sites. The capability to control the distribution of the emission region in single layer small-molecule OLEDs is considered to be a benefit over single layer PLEDs, in which the extent of the emission region is generally unmodifiable. The EL spectrum of Device B is identical to the multilayer Device A as shown in Figure 3. A maximum luminance of 33000 cd/m^2 was obtained at 16.5 V. As

shown in Figure 4(b), the maximum external quantum efficiency is 12.6% photon/electron (11.5 cd/A) and the maximum power efficiency is 7.8 lm/W. The efficiencies remain above 11.1% at the practical brightness of 100 cd/m^2. It can be observed that the efficiencies of the single layer Device B is reduced to about 70% of that of the multilayer Device A. A possible reason is unbalanced carrier injection, which may be overcome by further optimization of the carrier injection interfaces. Nevertheless, such performances are indeed impressive for a single layer device.

3. Summary

In summary, high-efficiency red phosphorescent OLEDs employing a novel red emitter qazIr(acac) and a multifunctional oligofluorene host SSS are reported. Using such new materials, red phosphorescent OLEDs with nearly 100% internal quantum efficiency are achieved. With qazIr(acac) as the red phosphorescent dopant, a maximum external quantum efficiency of 18.8% and maximum power efficiency of 10.5 lm/W were achieved. The CIE1931 coordinates of the saturated red device is (0.661, 0.336), and the maximum luminance is 32000 cd/m^2. In addition, due to the ambipolar carrier transporting properties of the oligofluorene host material and the judicious selection of carrier injection interfaces, highly efficient single layer small-molecule OLEDs are also demonstrated. Single layer devices using such host and dopant materials have efficiencies up to 12.6%. Such achievements not only contribute to the development of effective host and dopant materials for red phosphorescent OLEDs, but also to the simplification of device fabrication processes which is crucial in manufacturing.

4. Acknowledgements